Laser Photolysis of Caged Calcium: Rates of Calcium Release by Nitrophenyl-EGTA and DM-Nitrophen

Graham C. R. Ellis-Davies,‡ Jack H. Kaplan,* and Robert J. Barsotti‡
*Department of Biochemistry and Molecular Biology, Oregon Health Sciences University, Portland, Oregon 97201, and ‡Bockus Research Institute, Graduate Hospital, Philadelphia, Pennsylvania 19146 USA

ABSTRACT Nitrophenyl-EGTA and DM-nitrophen are Ca^{2+} cages that release Ca^{2+} when cleaved upon illumination with near-ultraviolet light. Laser photolysis of nitrophenyl-EGTA produced transient intermediates that decayed biexponentially with rates of 500,000 s^{-1} and 100,000 s^{-1} in the presence of saturating Ca^{2+} and 290,000 s^{-1} and 68,000 s^{-1} in the absence of Ca^{2+} at pH 7.2 and 25°C. Laser photolysis of nitrophenyl-EGTA in the presence of Ca^{2+} and the Ca^{2+} indicator Ca-orange-5N produced a monotonic increase in the indicator fluorescence, which had a rate of 68,000 s^{-1} at pH 7.2 and 25°C. Irradiation of DM-nitrophen produced similar results with somewhat slower kinetics. The transient intermediates decayed with rates of 80,000 s^{-1} and 11,000 s^{-1} in the presence of Ca^{2+} and 59,000 s^{-1} and 3,600 s^{-1} in the absence of Ca^{2+} at pH 7.2 and 25°C. The rate of increase in Ca^{2+}-indicator fluorescence produced upon photolysis of the DM-nitrophen: Ca^{2+} complex was 38,000 s^{-1} at pH 7.2 and 25°C. In contrast, pulses in Ca^{2+} concentration were generated when the chelator concentrations were more than the total Ca^{2+} concentration. Photoreleased Ca^{2+} concentration stabilized under these circumstances to a steady state within 1–2 ms.

INTRODUCTION

The rapid increase in intracellular Ca^{2+} concentration through the opening of Ca channels in the plasma membrane or sarco/endoplasmic recticulum is the signaling event that is responsible for the initiation of many physiological processes. For example, in the active zones of the neuron, it is Ca^{2+} binding to the secretory apparatus of the docked vesicles that stimulates membrane fusion and subsequent neurotransmitter release (Katz and Miledi, 1968; Heuser and Reese, 1981; Llinas et al., 1981; Heidelberger et al., 1994). In cardiac and skeletal muscle, it is the binding of Ca^{2+} to the regulatory protein troponin C that permits cross-bridge attachments to form and the force production to take place (Ebashi et al., 1969). Furthermore, it is Ca^{2+} binding to the ubiquitous protein calmodulin that is responsible for the regulation of a myriad of physiological events; e.g., G_2/M transition in the cell division cycle is controlled by the Ca^{2+}:calmodulin complex (Lu and Means, 1993).

We have recently developed a Ca^{2+} cage called nitrophenyl-EGTA (NP-EGTA) (Ellis-Davies and Kaplan, 1994), a photolabile Ca^{2+} chelator that can be used to increase the intracellular concentration of Ca^{2+} in the presence of physiological concentrations of Mg^{2+}. Ca^{2+} concentrations can thus be manipulated in cells without membrane depolarization and in preparations where the plasma membrane has been removed but in which traditional rapid mixing techniques are either too physically perturbing or do not provide adequate kinetic resolution for the processes under study. To be assured that the rate of cation release is not kinetically limiting when using this strategy in the study of Ca^{2+}-dependent physiological processes, the rate of cation photorelease must be determined.

In this report we use the low-affinity Ca^{2+} dye Ca-orange-5N to estimate the rate of release of Ca^{2+} upon laser flash photolysis of NP-EGTA saturated with Ca^{2+}. Furthermore, we have examined the time course of the free Ca^{2+} concentration when it is set initially to a nonactivating level for cellular processes. In addition to these measurements, the rates of decay of the photochromic reaction (or *aci*-nitro) intermediates intrinsic to the caged compound itself have been characterized (cf. Scheme 1). We have also reexamined our "first generation" Ca^{2+} cage, DM-nitrophen (Kaplan and Ellis-Davies, 1988; Ellis-Davies and Kaplan, 1988), in a similar series of experiments, so as to take advantage of superior temporal resolution of the flash photolysis apparatus and Ca^{2+} indicator used in this report. These measurements were made to determine whether the rate of decay of *aci*-nitro intermediates corresponds to the rate-limiting step in chelator fragmentation and Ca^{2+} release. Such measurements are vital for the successful use of our Ca^{2+} cages in physiological studies. Furthermore, they could also help in the interpretation of the photophysics of the majority of other *ortho*-nitrobenzyl caged compounds (review: Kao and Adams, 1993) for which the only currently available method of measuring the rate of caged compound release is through monitoring the rates of *aci*-nitro transient decay.

At physiological pH we have found that laser photolysis of NP-EGTA:Ca^{2+} complex generates two intermediates, which decay at rates of 500,000 and 100,000 s^{-1}, and that Ca^{2+} is released at a rate of at least 68,000 s^{-1}. Irradiation of DM-nitrophen evidenced slower signals: the *aci*-nitro species decay at rates of 80,000 and 11,000

Received for publication 27 April 1995 and in final form 27 October 1995.
Address reprint requests to Dr. Graham C. R. Ellis-Davies, Bockus Research Institute, 415 S. 19th Street, Philadelphia, PA 19146. Tel.: 215-893-2368; Fax: 215-893-4178.

0006-3495/96/02/1006/11 $2.00

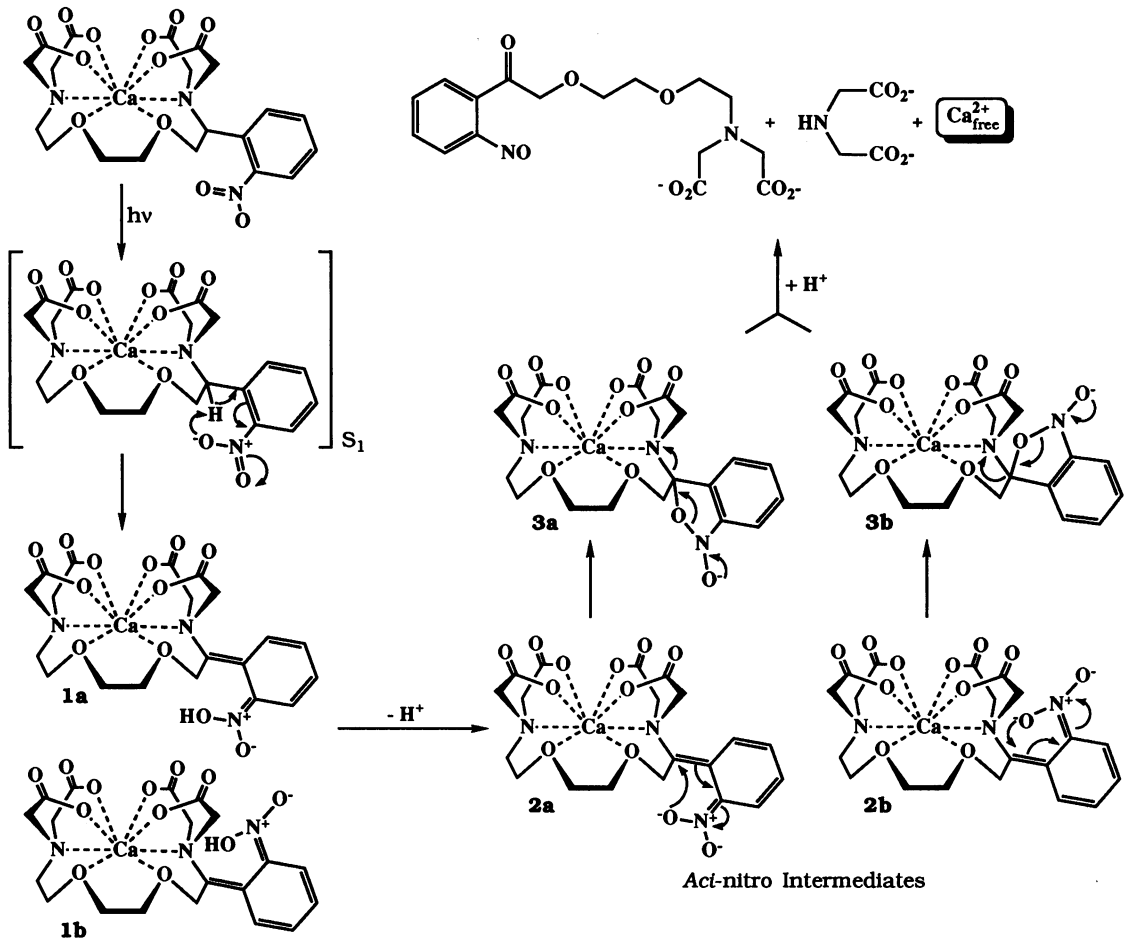

SCHEME 1 Photochemical reaction mechanism of nitrophenyl-EGTA.

s^{-1} and the dye shows Ca^{2+} is released at a rate of at least 38,000 s^{-1}. The simplest explanation of these data is that chelator fragmentation takes place along two parallel pathways, via *cis* and *trans aci*-nitro species. Ca^{2+} is, however, released either at the point of photocleavage or from the post-photolysis cation:products complex. A model is presented that is used to predict the free Ca^{2+} concentration waveform when the steady-state Ca^{2+} concentration is changed from nonactivating to activating levels by a single laser pulse.

MATERIALS AND METHODS

Materials

Nitrophenyl-EGTA and DM-nitrophen were synthesized according to our published methods (Ellis-Davies and Kaplan, 1988, 1994). Ca-orange-5N (lot no. C6770) was from Molecular Probes (Eugene, OR). $CaCl_2$, KCl, and KOH were of AR grade from BDH (Poole, Dorset, England). HEPES, 2[*N*-morpholino]ethanesulfonic acid (MES), and *N*-Tris[hydroxymethyl]methyl-3-amino-propanesulfonic acid (TAPS) were from Sigma (St. Louis, MO).

Indicator affinity

The dissociation constant of the 1,2-bis(aminophenoxy)ethane-*N*,*N*,*N*′,*N*′-tetraacetic acid (BAPTA)-based indicator Ca-orange-5N for Ca^{2+} was determined by titration of 1.0 mM solution of indicator in buffer (100 mM KCl, 50 mM HEPES, pH 7.2, 25°C) with incremental additions of Ca^{2+}. Fluorescence measurements were made on a Perkin-Elmer LS-50 spectrophotometer: excitation wavelength of 520 nm and emission scanned 550–650 nm. The intensity data were fitted by an equation assuming 1:1 binding between Ca^{2+} and indicator.

Flash photolysis

The photolysis reaction was initiated by a Q-switched ruby laser (Synergie Laser, Boca Raton, FL). The output (694 nm) was frequency doubled by passage through a potassium dihydrogen phosphate (KDP) crystal. The primary 694-nm output was separated from the secondary output by a Brewster stack polarizer and a UG-11 filter placed between the KDP crystal and the sample. This configuration produced a 35-ns, 150-mJ pulse of light with a wavelength of 347 nm. For the absorbance measurements, this light was focused by a cylindrical lens onto a 10 × 2 mm fluorescence quartz cuvette. The final beam size was approximately 8 × 1.5 mm. The absorbance changes were monitored at right angles to the photolysis beam. The light source for the absorbance measurements was an argon laser (model 5500A; Ion Laser Technology, Salt Lake City, UT) tuned to

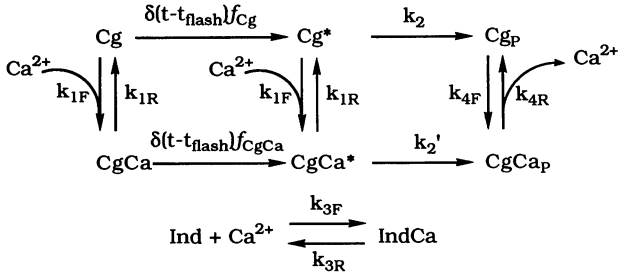

SCHEME 2 Kinetic scheme for modeling the rate of Ca^{2+} release upon photolysis of caged Ca^{2+}.

produce a 100-mW, 458-nm light beam with a diameter of approximately 0.8 mm. The beam intensity was attenuated using one neutral density filter (OD = 2) and a compensated attenuator (model 925B; Newport Corporation, Irvine, CA). The detection was via a photomultiplier (model 9601B; Thorn EMI, Rockaway, NJ) with a GG400, BG39 and a 450DF20 filter (Omega Optical, Brattleboro, VT) in front. The photocurrent was amplified by a custom built current to voltage preamplifier. The bandwidth of the detection system with the preamplifier was at least 5 MHz.

Fluorescence measurements

These were carried out by focusing the photolysis laser onto the stage of a Nikon diaphot epifluorescence microscope equipped with a custom-built rotating trough assembly. For these experiments, a 7-μl fused quartz trough (3 × 3 × 0.8 mm) was constructed using ESCO S1-UV fused silica (Esco Products, Oakridge, NJ) and mounted on the stage assembly. The optical components included a 75-W xenon light source (Nikon); a Zeiss Neofluar objective (6.3 × magnification, N.A. = 0.2); an excitation filter (488DF20); dichroic 505 DRLP; and an emission filter (570DF20; Omega Optical); and a GG400 filter placed before the photomultiplier (model 9924B; Thorn EMI). The data in all experiments were digitized and stored on a digital oscilloscope (model 9304; Le Croy Corp., Chestnut Ridge, NY). The data were digitized at a maximum rate of 50 MHz. The Ca^{2+} pulses monitored by the fluorescence of Ca-orange-5N were fit to the model shown in Scheme 2 using the Davidson-Fletcher-Powell algorithm (Press et al., 1992).

EQUATIONS

Modeling

Scheme 2 depicts a simplified reaction pathway for the photolysis of caged Ca^{2+} and the interaction of free Ca^{2+} with the unphotolyzed and photolyzed forms. The scheme also includes the interaction of free Ca^{2+} with a fluorescent Ca^{2+} indicator. The reaction scheme can be described by the following set of equations:

$$\frac{d[Cg]}{dt} = -k_{1F}[Cg][Ca^{2+}] + k_{1R}[CgCa] - \delta(t - t_{flash})f_{Cg}[Cg] \quad (1)$$

$$\frac{d[CgCa]}{dt} = k_{1F}[Cg][Ca^{2+}] - k_{1R}[CgCa] - \delta(t - t_{flash})f_{CgCa}[CgCa] \quad (2)$$

$$\frac{d[Cg^*]}{dt} = k_{1F}[Cg^*][Ca^{2+}] + k_{1R}[CgCa^*] + \delta(t - t_{flash})f_{Cg}[Cg] - k_2[Cg^*] \quad (3)$$

$$\frac{d[CgCa^*]}{dt} = k_{1F}[Cg^*][Ca^{2+}] - k_{1R}[CgCa^*] + \delta(t - t_{flash})f_{CgCa}[CgCa] - k_2'[CgCa^*] \quad (4)$$

$$\frac{d[Cg_P]}{dt} = k_{4F}[Cg_P][Ca^{2+}] - k_{4R}[CgCa_P] + 2k_2[Cg^*] + k_2'[CgCa^*] \quad (5)$$

$$\frac{d[CgCa_P]}{dt} = k_{4F}[Cg_P][Ca^{2+}] - k_{4R}[CgCa_P] + k_2'[CgCa^*] \quad (6)$$

$$\frac{d[Ind]}{dt} = -k_{3F}[Ind][Ca^{2+}] + k_{3R}[IndCa] \quad (7)$$

$$\frac{d[IndCa]}{dt} = -\frac{d[Ind]}{dt}. \quad (8)$$

[Cg] is the [DM-nitrophen] or [NP-EGTA] and [CgCa] the concentration of their Ca^{2+} complexes. [Cg_P] and [$CgCa_P$] represent the concentration of photoproducts without and with Ca^{2+}. The concentrations of free and Ca^{2+}-bound indicator are denoted as [Ind] and [IndCa]. [Cg*] and [CgCa*] are the concentrations of chelators without and with Ca^{2+}, respectively, that photo-fragment to form prod-

TABLE 1 Rates of *aci*-nitro intermediate decay of and Ca^{2+} release from nitrophenyl-EGTA

pH	*Aci*-nitro decays (s^{-1})		Ca^{2+} release rates* (s^{-1})
	$+Ca^{2+}$	$-Ca^{2+}$	
6.2	$6.2 \pm 1.8 \times 10^5$ (60%) $2.9 \pm 0.95 \times 10^5$	ND	$6.5 \pm 0.42 \times 10^4$
7.2	$5.0 \pm 0.91 \times 10^5$ (63%) $1.0 \pm 0.68 \times 10^5$	$2.9 \pm 0.36 \times 10^5$ (60%) $6.8 \pm 3.8 \times 10^4$	$6.8 \pm 0.40 \times 10^4$
8.2	$2.5 \pm 0.15 \times 10^5$ (80%) $2.0 \pm 0.66 \times 10^4$	$2.2 \pm 0.32 \times 10^5$ (65%) $2.6 \pm 1.6 \times 10^4$	$6.3 \pm 0.56 \times 10^4$

The values represent the average of six to ten experiments, and are shown ±SD. The relative contribution of the fast component to the transient signal is shown in parentheses.

*These rates are only a lower estimate as the response of the indicator may be rate limiting in these measurements.

TABLE 2 Rates of *aci*-nitro intermediate decay of and Ca^{2+} release from DM-nitrophen

pH	*Aci*-nitro decays (s^{-1})		Ca^{2+} release rates* (s^{-1})
	$+Ca^{2+}$	$-Ca^{2+}$	
6.2	$7.1 \pm 0.51 \times 10^4$ (76%) $7.6 \pm 4.3 \times 10^3$	$4.0 \pm 0.78 \times 10^4$ (88%) $6.3 \pm 5.1 \times 10^3$	$4.1 \pm 0.53 \times 10^4$
7.2	$8.0 \pm 0.79 \times 10^4$ (66%) $1.1 \pm 0.39 \times 10^4$	$5.9 \pm 0.62 \times 10^4$ (80%) $3.6 \pm 0.99 \times 10^3$	$3.8 \pm 0.32 \times 10^4$
8.2	$3.5 \pm 0.31 \times 10^4$ (57%) $3.9 \pm 2.9 \times 10^3$	$3.9 \pm 0.49 \times 10^4$ (55%) $2.9 \pm 1.1 \times 10^3$	$4.4 \pm 0.67 \times 10^4$

The values represent the average of six to ten experiments, and are shown ±SD. The relative contribution of the fast component to the transient signal is shown in parentheses.

*These rates are only a lower estimate as the response of the indicator may be rate limiting in these measurements.

ucts. Cg* and CgCa* are a convenient way to distinguish mathematically the fractions of free and Ca^{2+}-bound cage from the remaining unphotolyzed fractions. $\delta(t - t_{flash})$ is a Dirac delta "function" that is used to model the instantaneous conversion of fractions f_{Cg} and f_{CgCa} of Cg and CgCa to Cg* and CgCa*, which then decay with rate constants k_2 and k_2', respectively, to photoproducts: Cg_P and $CgCa_P$. Although we show that the rate of decay of the *aci*-nitro intermediates is slower in the absence of Ca^{2+} than its presence (Tables 1 and 2), this difference is less than a factor of 2. Furthermore, because a majority of each cage is complexed with Ca in these experiments, the predominate flux pathway will be via CgCa*. Thus, for simplicity, in all numerical calculations we have set $k_2 = k_2'$. k_F and k_R are rate constants for Ca^{2+} binding to the various forms of the cage and the indicator.

The time course of the change in fluorescence due to Ca^{2+} binding to the indicator was monitored after laser photolysis of Ca^{2+} complexes of NP-EGTA and DM-nitrophen (see Figs. 5 and 6). Equations 1–8 were programmed into a PC so that the data from photolysis experiments could be fitted to determine intrinsic rate constants. The resulting information was then used to predict the time course of the free $[Ca^{2+}]$ after photolysis. Experimental conditions were selected such that a transient increase in free $[Ca^{2+}]$ was produced, i.e., initially $[Cg] > [Ca^{2+}]$ (see Figs. 5 and 6). Estimates of the rate constants for Ca^{2+} binding to the cage and indicator were derived by fitting the time course of fluorescence with the model. During fitting, values for all parameters were fixed except k_{1R} and k_{3R}. These were fit with the condition that K_{1D} and K_{3D} were constant (the values are listed in Table 3), and k_{1F} and k_{3F} were equal to k_{1R}/K_{1D} and k_{3R}/K_{3D}. The values for the remaining parameters used to fit the fluorescence time course are shown in Table 3. Note that the photolysis of one molecule of Cg* results in the formation of two molecules of Cg_P, and the photolysis of one molecule of CgCa* results in the formation of one molecule of Cg_P and one molecule of $CgCa_P$. This is described in the last two terms on the right-hand side of Eq. 5. Furthermore, modeling was performed under the assumption that the quantum yield of photolysis of Ca^{2+}-bound cage and free cage are the same (cf. Ellis-Davies and Kaplan, 1994). Estimates of the fractions of cage photolyzed (f_{Cg} and f_{CgCa}) were determined from the change in steady-state $[Ca^{2+}]$, which was estimated from the net change in fluorescence of Ca-orange-5N (following the correction methods of Kao et al., 1989). The amount of photobleaching of the indicator by the laser pulse was negligible. The resulting information was then used to predict the time course of free $[Ca^{2+}]$ after photolysis.

Speed of Ca^{2+}:indicator interactions

Ca-orange-5N binds Ca^{2+} with a 1:1 stoichiometry, as shown in Scheme 2. Therefore, the changes in [CaInd], i.e.,

TABLE 3 Rate constants, dissociation constants, and variables for scheme 2

Constant	DM-nitrophen	NP-EGTA	Source of value
k_{1F}	$8 \times 10^7\ M^{-1}\ s^{-1}$	$1.7 \times 10^7\ M^{-1}\ s^{-1}$	k_{1R}/k_{1D}
k_{1R}	$0.40\ s^{-1}$	$1.36\ s^{-1}$	Fit with model
k_2	$8 \times 10^4\ s^{-1}$	$4.5 \times 10^5\ s^{-1}$	Faster *aci*-nitro decay of cage
k_{3F}	$3 \times 10^8\ M^{-1}\ s^{-1}$	$3 \times 10^8\ M^{-1}\ s^{-1}$	k_{3F}/K_{3D}
k_{3R}	$1.26 \times 10^4\ s^{-1}$	$1.26 \times 10^4\ s^{-1}$	Fit with model
k_{4F}	$8.0 \times 10^7\ M^{-1}\ s^{-1}$	$8.0 \times 10^7\ M^{-1}\ s^{-1}$	Set equal to k_{1F}
k_{4R}	$2.4 \times 10^4\ s^{-1}$	$8.0 \times 10^5\ s^{-1}$	k_{4F}/K_{4D}
K_{1D}	5×10^9 M	8.0×10^{-8} M	DM-nitrophen: Kaplan and Ellis-Davies, 1988
K_{4D}	3.0×10^{-3} M	1.0×10^{-3} M	NP–EGTA: Ellis-Davies and Kaplan, 1994
$[Cg]_{Total}$	2.2 mM	2.0 mM	Total added
$[Ind]_{Total}$	50 μM	50 μM	Total added
$[Ca]_{Total}$	1.8 mM	1.7 mM	Total added
$f_{Cg} = f_{CgCa}$	0.16	0.13	See text

the signal monitored in the experiments shown in Figs. 3–6, should follow:

$$\frac{d[CaInd]}{dt} = k_{3F}[Ca][Ind] - k_{3R}[CaInd], \quad (9)$$

where [Ca] is the free Ca^{2+} concentration, [Ind] is the free indicator concentration, and [CaInd] is the concentration of the Ca^{2+}:indicator complex.

If the free Ca^{2+} concentration is perturbed from its steady state to a new, higher level, then [CaInd] increases according to Eq. 9. Because [Ind] + [CaInd] is constant, the increase in [CaInd] follows an exponential time course, with a rate constant k_{app}, given by

$$k_{app} = k_{3F}[Ca] + k_{3R}. \quad (10)$$

If [Ca^{2+}] is much less than the dissociation constant of the indicator, then the first term on the right-hand side of Eq. 10 can be neglected, i.e., the off rate (k_{3R}) of the indicator defines the kinetic limit of the signal monitored. However, with increasing amounts of Ca^{2+}, this first term (k_{3F}[Ca]) must be taken into account, i.e., the on rate plays an important role in the overall signal detected (cf. Baylor et al., 1982; Kao and Tsien, 1988).

RESULTS

Two types of time-dependent measurements were made to obtain information on the rate of release of Ca^{2+} from NP-EGTA and DM-nitrophen. It is well known that flash photolysis of *o*-nitrobenzyl compounds at 350 nm produces transient intermediates (or *aci*-nitro species; cf. structures 1 and 2 in Scheme 1) that absorb at 450 nm (Wettermark, 1962; McCray et al., 1980, 1992; Schupp et al., 1987; McClelland and Steenken, 1987). A single pulse from a frequency-doubled ruby laser (150 mJ at 347 nm) generated such *aci*-nitro species, the rate of disappearance of which was probed with the 458-nm line of an argon laser. NP-EGTA exhibited *aci*-nitro signals over the entire pH range tested, which were fitted to a double exponential equation. At physiological pH the decay rates were 500,000 s^{-1} and 100,000 s^{-1} in the presence of Ca^{2+} and 290,000 s^{-1} and 68,000 s^{-1} in the absence of Ca^{2+} (see Fig. 1). Irradiation of DM-nitrophen produced similar signals, as shown in Fig. 2. The rates of decay at pH 7.2 were 80,000 s^{-1} and 11,000 s^{-1} with Ca^{2+} and 59,000 s^{-1} and 3,600 s^{-1} without Ca^{2+}. *Aci*-nitro intermediate decay rates for both Ca^{2+} cages in the presence and absence of Ca^{2+} for pH 6.2–8.2 are summarized in Tables 1 and 2.

Laser flash photolysis (150 mJ at 347 nm) of NP-EGTA (2 mM) in the presence of saturating Ca^{2+} (2.1

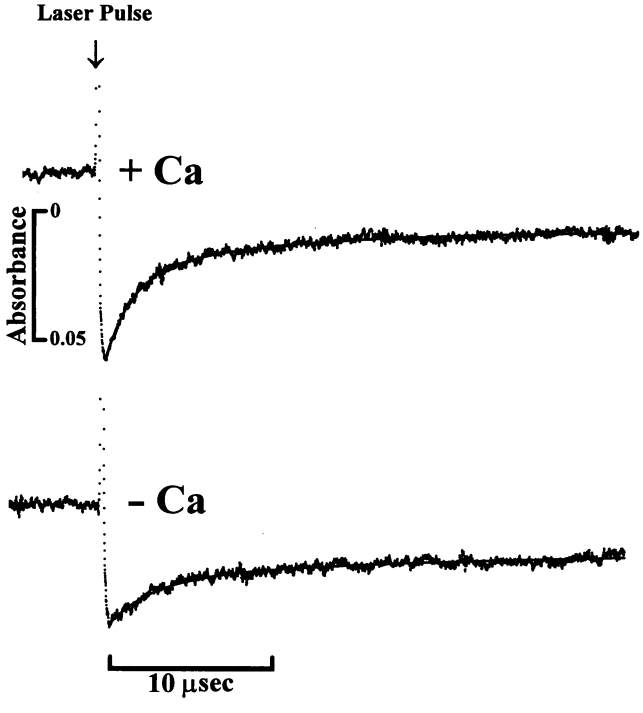

FIGURE 1 Nitrophenyl-EGTA *aci*-nitro transient intermediates. A single pulse from a frequency-doubled ruby laser (347 nm, 150 mJ) was used to photolyze a solution of NP-EGTA (2.0 mM) in the presence (2.1 mM) and absence of Ca^{2+} at pH 7.2 (40 mM HEPES) with 100 mM KCl at 25°C. The absorption transients were monitored at 458 nm. The declining phase of the signal was fit to a double exponential expression plus a constant, and the resultant values were used to calculate the solid curves overlaid on each trace.

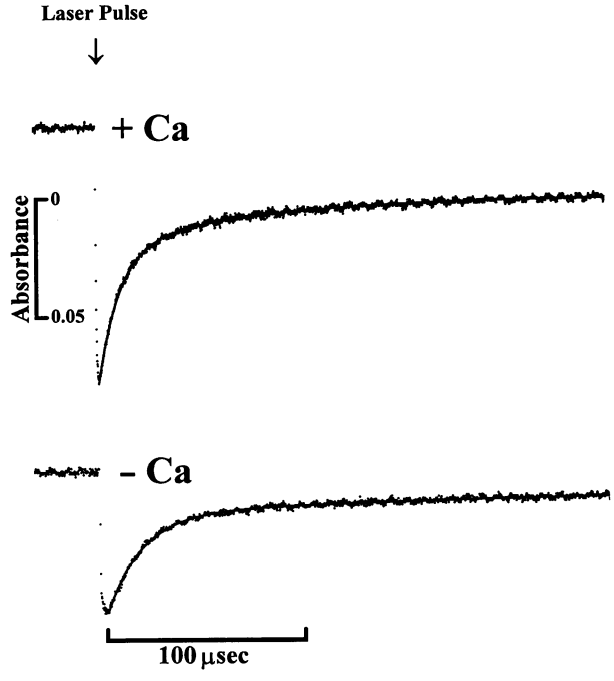

FIGURE 2 DM-nitrophen *aci*-nitro transient intermediates. A single pulse from a frequency-doubled ruby laser (347 nm, 150 mJ) was used to photolyze a solution of DM-nitrophen (2.0 mM) in the presence (2.1 mM) and absence of Ca^{2+} at pH 7.2 (40 mM HEPES) with 100 mM KCl at 25°C. The absorption transients were monitored at 458 nm. The declining phase of the signal was fit to a double exponential expression plus a constant, and the resultant values were used to calculate the solid curves overlaid on each trace.

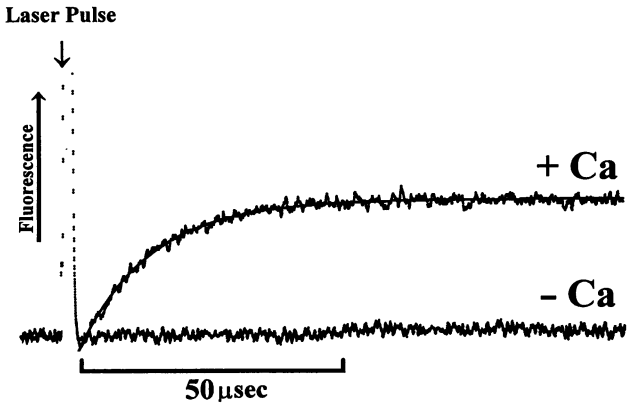

FIGURE 3 Time-dependent increase in fluorescence of Ca-orange-5N upon photolysis of nitrophenyl-EGTA:Ca^{2+}. A single pulse from a frequency-doubled ruby laser (347 nm, 150 mJ) was used to photolyze a solution of NP-EGTA (2.0 mM) in the presence of Ca^{2+} (2.1 mM) at pH 7.2 (40 mM HEPES) with 100 mM KCl at 25°C. The fluorescence signal from Ca-orange-5N (50 μM) was monitored: excitation 488 ± 10 nm, emission 570 ± 10 nm. The traces represent an average of five recordings. The averaged signal was fit to a single exponential expression plus a constant, and the resultant values were used to calculate the solid curve overlaid on the trace.

mM) at physiological pH elicited the time-dependent increase in fluorescence of the indicator Ca-orange-5N (50 μM) shown in Fig. 3, which could be fitted with a monoexponential rate constant of 68,000 s^{-1}. A value of 38,000 s^{-1} was obtained for DM-nitrophen under similar conditions (Fig. 4). The indicator was excited at 488 ± 10 nm, and emission was monitored at 575 ± 10 nm from a small trough mounted on an epifluorescent microscope. There is a large laser-induced transient spike in this measurement system, which is of short enough duration so as not to interfere with the indicator signal. Both Ca^{2+} cages were found to release Ca^{2+} with rates in the 38,000 to 68,000 s^{-1} range over the entire pH range studied. These data are summarized in Tables 1 and 2.

The response of Ca-orange-5N to photolysis of the Ca^{2+} cages in the presence of nonsaturating concentrations of Ca^{2+} is shown in Figs. 5 and 6. In both cases a pulse of Ca^{2+} was produced; the Ca^{2+} concentration stabilized to 105% of the new steady-state value in about 1–2 ms. These pulses have been fit to the reaction mechanism shown in Scheme 2, assuming chelators are cleaved at a rate corresponding to the faster of the two *aci*-nitro transient decays. Only two parameters were allowed to vary in the fit, k_{1R}, the off rate of Ca^{2+} from the unphotolyzed cage (Cg), and k_{3R}, the off rate from the indicator (IndCa); starting values for k_{1F} could be selected to be either diffusion limited ($6 \times 10^8\ M^{-1}\ s^{-1}$) or similar to EGTA ($1.5 \times 10^6\ M^{-1}\ s^{-1}$). In either case, the fit converged to yield the values shown in Table 3. The on rate of Ca^{2+} (k_{4F}) to the photoproducts of both NP-EGTA and DM-nitrophen (Cg_P) was held to the same value as the on rate for Ca^{2+} (k_{1F}) binding to unphotolyzed DM-nitrophen. Unphotolyzed DM-nitrophen provides the most reasonable estimate of the pK_a of the photoproducts (because they are all only singly protonated at physiological pH), and so k_{4R} is derived from the

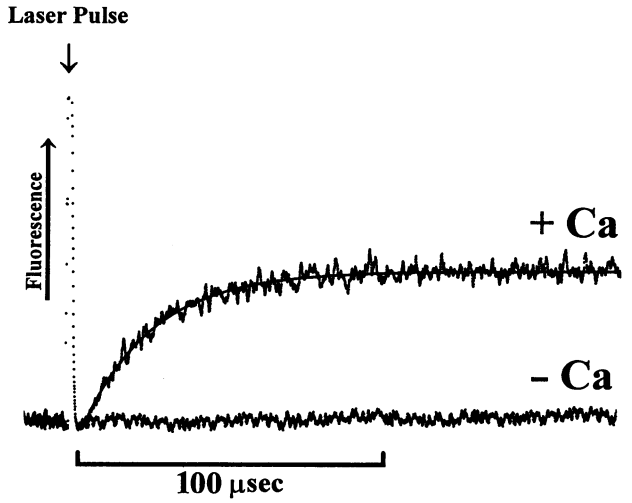

FIGURE 4 Time-dependent increase in fluorescence of Ca-orange-5N upon photolysis of DM-nitrophen:Ca^{2+}. A single pulse from a frequency-doubled ruby laser (347 nm, 150 mJ) was used to photolyze a solution of DM-nitrophen (2.0 mM) in the presence of Ca^{2+} (2.1 mM) at pH 7.2 (40 mM HEPES) with 100 mM KCl at 25°C. The fluorescence signal from Ca-orange-5N (50 μM) was monitored: excitation 488 ± 10 nm, emission 570 ± 10 nm. The traces represent an average of five recordings. The averaged signal was fit to a single exponential expression plus a constant, and the resultant values were used to calculate the solid curve overlaid on the trace.

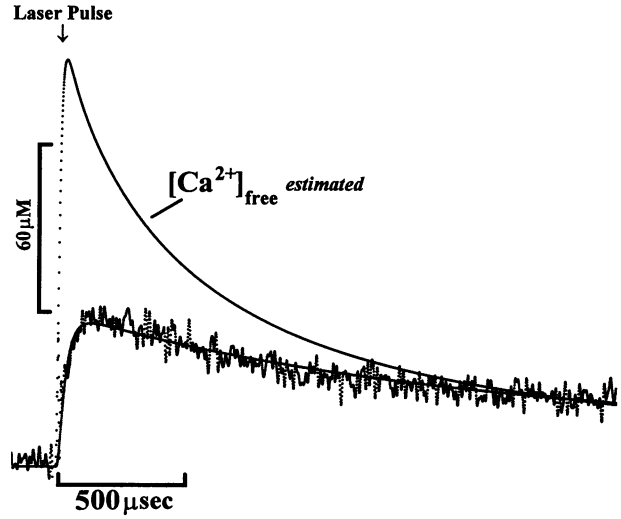

FIGURE 5 Ca^{2+} concentration pulse upon photolysis of nitrophenyl-EGTA:Ca^{2+}. A single pulse from a frequency-doubled ruby laser (347 nm, 150 mJ) was used to photolyze a solution of NP-EGTA (2.0 mM) in the presence of Ca^{2+} (1.7 mM) at pH 7.2 (40 mM HEPES) with 100 mM KCl at 25°C. The fluorescence signal (noisy trace) from Ca-orange-5N (50 μM) was monitored: excitation 488 ± 10 nm, emission 570 ± 10 nm. This signal was fitted to Scheme 2 as described in the equations, and the resultant trace is shown (*solid line*). The $[Ca^{2+}]_{free}$ waveform was calculated from these data and is shown in the upper curve.

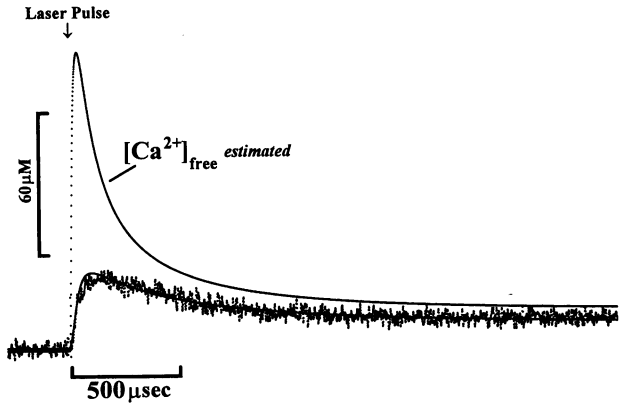

FIGURE 6 Ca^{2+} concentration pulse upon photolysis of DM-nitrophen: Ca^{2+}. A single pulse from a frequency-doubled ruby laser (347 nm, 150 mJ) was used to photolyze a solution of DM-nitrophen (2.3 mM) in the presence of Ca^{2+} (1.8 mM) at pH 7.2 (40 mM HEPES) with 100 mM KCl at 25°C. The fluorescence signal (noisy trace) from Ca-orange-5N (50 μM) was monitored: excitation 488 ± 10 nm, emission 570 ± 10 nm. This signal was fitted to Scheme 2 as described in the equations, and the resultant trace is shown (*solid line*). The $[Ca^{2+}]_{free}$ waveform was calculated from these data and is shown in the upper curve.

known K_D values of the photoproducts of NP-EGTA and DM-nitrophen. Based on the values for these rate constants obtained from the fitting procedure and from the determined K_D values for the cages and indicator, the values for both k_{1F} and k_{3F} could be calculated. These values, along with the other parameters listed in Table 3, were used to model the $[Ca^{2+}]_{free}$ waveform shown in the upper curves of Figs. 5 and 6. In the case of NP-EGTA, the initial value of $[Ca^{2+}]_{free}$ = 450 nM if $[NP\text{-}EGTA]_{total}$ = 2 mM and $[Ca^{2+}]_{total}$ = 1.7 mM. Thirteen percent photolysis of the chelator changes the $[Ca^{2+}]_{free}$ to a new steady state of 17 μM, and the waveform in Fig. 5 predicts that the $[Ca^{2+}]_{free}$ reaches a maximum value of 139 μM after 45 μs. For DM-nitrophen (2.2 mM), similar calculations were performed, except that $[Ca^{2+}]_{total}$ = 1.8 mM and 16% was photolyzed, giving a maximum value of $[Ca^{2+}]_{free}$ = 124 μM after 34 μs (Fig. 6).

DISCUSSION

Laser flash photolysis has been used to obtain an estimate of the rate of cation release from our two caged calciums (DM-nitrophen, Ellis-Davies and Kaplan, 1988; Kaplan and Ellis-Davies, 1988; and NP-EGTA, Ellis-Davies and Kaplan, 1994). Furthermore, the rates corresponding to the decay of intermediates along the chelator fragmentation pathway for each cage have been measured. These were made to determine whether there is any correlation between the rate of Ca^{2+} release and the decay of the NP-EGTA and DM-nitrophen *aci*-nitro intermediates.

The primary photochemical process of electronically excited *ortho*-nitrotoluenes is benzylic proton abstraction (Morrison and Migdalof, 1965). It is this reaction that is responsible for the deexcitation of the chromophore via π-electron reorganization to the ground-state *aci*-nitro intermediate. If the benzylic carbon bears a hetro atom (N in the case of NP-EGTA and DM-nitrophen), then these highly energetic intermediates relax by bond rupture and concomitant release of the caged substrate. This relaxation is often referred to as the "dark reaction" in caged compound literature. Only in the case of certain caged nucleotides has it been shown that the disappearence of *aci*-nitro absorption occurs with the same rate as the release of the caged substrate (caged ATP: McCray et al., 1980; Walker et al., 1988; caged ϵ-azaATP and cFMP: Wootton and Trentham, 1989). For many other caged compounds this has been assumed to be the case (Walker et al., 1986, 1989; Khan et al., 1993; Corrie, 1993; Weiboldt et al., 1994; Wilcox et al., 1990; Ramesh et al., 1993; Milburn et al., 1989; Billington et al., 1992). In the case of the nitr Ca^{2+} cages the appearance of the organic photoproduct has been used to estimate the rate of Ca^{2+} release (Adams et al., 1988). However, in some of these cases two *aci*-nitro intermediates have been observed (Milburn et al., 1989; Ramesh et al., 1993; Corrie, 1993; Weiboldt et al., 1994). In a few cases the rate of appearance of the proton side-product, which results from the irradiation of some *ortho*-nitrobenzyl caged compounds, has been used to estimate the rate of product appearance after laser photolysis of these caged compounds. In the case of caged ATP (Walker et al., 1988), caged P_i (Dantzig et al., 1992) and caged glutamate (Corrie et al., 1993), the decay of the intermediate that produces the *aci*-nitro transient absorption occurs at the same rate as the appearance of a signal from a pH indicator.

There are two hypotheses concerning how Ca^{2+} is released from a photolabile chelator. These lie at the extremes of a spectrum of possible reaction mechanisms that can be used to describe the photolysis of NP-EGTA and DM-nitrophen and so rationalize the data presented in this report. The first is that upon fracture of the chelator backbone, Ca^{2+} is released: thus the decay of the *aci*-nitro intermediates will be concomitant with the appearance of Ca^{2+}. Alternatively, the rate-limiting step in chelator fragmentation and the rate of Ca^{2+} release could be different. That is, caged Ca^{2+} is photolyzed at a rate corresponding to the decay of the *aci*-nitro intermediates to give photoproducts still bearing Ca^{2+}, and these Ca^{2+}-dicarboxylate photoproduct complexes then release Ca^{2+} at a rate dictated by their dissociation rate constant.

The use of an independent means of monitoring the rate of release from a caged compound other than caged ATP (Walker et al., 1988) could aid the understanding of *ortho*-nitrobenzyl caged compounds for which indicators are not available to monitor the appearence of the caged compound. In this report we present evidence that, in the case of DM-nitrophen, the rate of decay of the *aci*-nitro transient intermediates can be associated with the rate of release of the caged Ca^{2+}. Thus, we not only provide kinetic data for the use of this specific caged compound but also strengthen the hypothesis that the rate of *aci*-

nitro transient decay is an indication of the rate of *ortho*-nitrobenzyl caged compound photorelease in general.

Nitrophenyl-EGTA and DM-nitrophen *aci*-nitro decays are biphasic

Laser flash photolysis of the NP-EGTA:Ca^{2+} complex results in transient *aci*-nitro intermediates similar to those of all other *o*-nitrobenzyl caged compounds. It was found, however, that the decay rates were at least an order of magnitude faster than any previously reported for *o*-nitrobenzyl caged compounds. At physiological pH, NP-EGTA evidenced two *aci*-nitro intermediates, which decayed at rates of 500,000 and 100,000 s^{-1} when saturating concentrations of Ca^{2+} were present. There have been several reports in the literature of such phenomena. In fact, most other functional groups show analogous behavior: caged ethers (Corrie, 1993), carboxylates (Zhu et al., 1987; Wieboldt et al., 1994), carbamates (Milburn et al., 1989), amides (Ramesh et al., 1993), and amines (McCray et al., 1992) have all been reported to show two *aci*-nitro intermediates. A notable exception to this are substrates containing a caged phosphate functionality (McCray et al., 1980; Walker et al., 1988, 1989; Wootton and Trentham, 1989; Khan et al., 1993): the *aci*-nitro transients generated upon laser photolysis of a wide variety of such compounds (e.g., ATP, P_i, IP_3, cAMP, etc.) can be consistently fitted to a monoexponential decay.

There are several possible interpretations of the biphasic nature of *aci*-nitro transient intermediates. For example, Schnabel and co-workers have made a detailed investigation of the photochemical reaction mechanism of caged carboxylates using time-resolved absorption conductivity and resonance Raman measurements (Schupp et al., 1987; Zhu et al., 1987; cf. Schneider et al., 1991). They have found that the conjugate acid *aci*-nitro intermediates (nitronic acids of type 1) decay with half-times of 3 μs to their conjugate base (or nitronate anions of type 2). This species then decays to products via the bridged intermediate of type 3 with a half-time of 10 ms (the solvent was 60% ethanol, 40% H_2O). McClelland and Steenken (1987) have found that the *aci*-nitro conjugate acid has a very brief half-time in aqueous solution. In their experiments the conjugate base was formed in the lifetime of the laser pump pulse (35 ns). However, in acetonitrile the conjugate acid had a lifetime of 100 μs. Thus, it would seem that in the case of NP-EGTA the conjugate base, *aci*-nitro intermediate 2, would be formed very rapidly (within the 35-ns laser pulse), as all our studies were performed in a fully aqueous medium.

Schnabel et al. have also suggested that biexponential *aci*-nitro decay could be caused by the formation of cisoid and transoid intermediates (Zhu et al., 1987). This seems the most plausible explanation of the observed biexponential decay of *aci*-nitro intermediates in the case of both NP-EGTA and DM-nitrophen. Thus, *aci*-nitro intermediates with structures 2a and 2b would give rise to the two signals we detected in the case of NP-EGTA.

The *aci*-nitro transient decays of DM-nitrophen were also found to be biexponential; the two intermediates decayed at rates of 80,000 s^{-1} and 11,000 s^{-1} at physiological pH when Ca^{2+} was present in the reaction medium. Our previous studies also showed biexponential decay of the *aci*-nitro intermediates of DM-nitrophen (McCray et al., 1992). For reasons we do not yet understand our current measuring system yields rates that are 3–4 times faster than our earlier measurements. The rates of decay of the DM-nitrophen:Ca^{2+} complex *aci*-nitro transients was found to be mildly pH dependent over the 6.2–8.2 range; the absence of Ca^{2+} resulted in little or no proton catalysis. Caged compounds show a variety of pH effects on the rate of *aci*-nitro decay. For example, caged P_i is fully pH catalyzed from pH 7–10 (Walker et al., 1988), whereas caged carbamylcholine shows only a factor of 2–3 in the same pH range (Walker et al., 1986). The rate of decay of *aci*-nitro intermediates of caged protons is fully pH catalyzed from pH 5.5 to 7.5 but only twofold from 7.5 to 10 (Khan et al., 1993). Thus, even though the reaction mechanism outlined in Scheme 1 is generally accepted as the means of caged compound release, the effect of pH on the rate of *aci*-nitro intermediate decay and on the rate-determining step of cage compound release varies depending on the substrate, so this scheme may in fact give a less than complete description of the reaction mechanism. The complexity of the intrinsic photochemistry of nitrophenyl-EGTA and DM-nitrophen illustrates the importance of the use of an independent means to determine the rate of release of the effector molecule from its caged precursor.

The rate of Ca^{2+} release: use of fluorophoric dyes

The primary aim of these investigations was to obtain an estimate of the rate of Ca^{2+} release by laser photolysis of the NP-EGTA:Ca^{2+} complex. Since the development of DM-nitrophen and our preliminary report of its Ca^{2+} release rate (Fidler et al., 1988) a number of new Ca^{2+} sensitive indicators have been developed. For example, the murexide-based dye purpurate-1,1′-diacetic acid (PDAA) would seem to possess many properties that would make it ideal for the quantitation of the $[Ca^{2+}]_{free}$ waveform that results from laser flash photolysis of both the NP-EGTA:Ca^{2+} and DM-nitrophen:Ca^{2+} complexes: namely, very low Ca^{2+} affinity (K_d = 1 mM), large $\Delta\epsilon$ upon Ca^{2+} binding (~13 mM^{-1} cm^{-1}), and absorption response to Ca^{2+} at 540 nm (Southwick and Waggoner, 1989). In particular, the low affinity made this indicator a very attractive candidate because this means that k_{off} is about 5×10^5 s^{-1} and thus this dye rapidly equilibrates upon a change in $[Ca^{2+}]$. Unfortunately all attempts to obtain a signal from PDAA by photolysis of NP-EGTA:Ca^{2+} complex failed because the *aci*-nitro transients have an absorption "tail" that overlaps with and masks the PDAA:Ca^{2+} transmission signal increase at 540 nm.

To circumvent this problem, we turned to a recently developed Ca^{2+} fluorophore, Ca-orange-5N, which is the lowest affinity BAPTA-based indicator available. This indicator was found to have a K_d of 43 μM. The modeling provided an estimate of k_{on} of 3×10^8 M^{-1} s^{-1} and thus of k_{off} of 1.26×10^4 s^{-1} (cf. for fura-2 the rate is 6×10^8 M^{-1} s^{-1} and azo-1 is 4×10^8 M^{-1} s^{-1} at 20°C; Kao and Tsien, 1988; cf. Jackson et al., 1987). Consequently, it would be predicted that Ca-orange-5N would not track the $[Ca^{2+}]_{free}$ with complete fidelity after laser-induced cation release, if the rate of Ca release is greater than 12,000 s^{-1}, because at rates greater than this the indicator:Ca complex is not at equilibrium (see Materials and Methods for the theoretical treatment). However, the indicator can monitor changes in $[Ca^{2+}]$ that are more rapid than this, as the rate of change of the fluorescence emission is sensitive to the initial $[Ca^{2+}]_{free}$, the amount of Ca released, and the indicator concentration. The more fully saturated the indicator is, the greater the contribution the on rate makes to overall signal (Eq. 10). This increased temporal resolution is balanced, however, by a loss in sensitivity due to the smaller fluorescence change produced under these conditions.

The rates of Ca^{2+} photorelease monitored with this indicator are in Tables 1 and 2 and show that the NP-EGTA:Ca^{2+} and DM-nitrophen:Ca^{2+} complexes release Ca^{2+} extremely rapidly upon irradiation with a 35-ns laser light pulse. At physiological pH, the rate of increase in fluorescence could be fitted to a monoexponential curve with a rate constant of 68,000 s^{-1} for NP-EGTA and 38,000 s^{-1} for DM-nitrophen. The slightly different rates reflect the subtle differences in experimental conditions in these two experiments; hence the time-dependent increase in fluorescence reported by the dye is not quite the same. Both are, however, probably at the kinetic limit of the dye for the individual experiment. The value for NP-EGTA is quite close to the estimate for the off rate of the photoproducts (k_{4R}, Scheme 2) obtained from modeling Ca^{2+} release of 80,000 s^{-1} (see below, Table 3). In the case of DM-nitrophen, the corresponding rate constant is estimated to be 240,000 s^{-1}, six times faster than the Ca^{2+} release rate reported by the indicator. This off rate would not be rate limiting though, as the faster *aci*-nitro decay rate is only 80,000 s^{-1}. Thus, bond breaking most probably defines the Ca^{2+} release rate for this Ca^{2+} cage.

The exact nature of the relationship between chelator fragmentation and Ca^{2+} release for the two cages cannot be settled definitively without a Ca^{2+} indicator that will provide better temporal resolution than those currently available. Nevertheless, Ca-orange-5N shows that both NP-EGTA and DM-nitrophen Ca^{2+} complexes photorelease Ca^{2+} extremely quickly, with half-times in the 10–20-μs time domain.

Calcium pulses from nitrophenyl-EGTA and DM-nitrophen

The Ca^{2+} release experiments described above were performed under conditions where the cages were fully saturated with Ca^{2+} and consequently the initial value of $[Ca^{2+}]_{free}$ would be activating for some physiological processes. Under these conditions the photoreleased Ca^{2+} very rapidly attains a new (higher) resting level, as the only available uncomplexed Ca^{2+} buffers are the cage photoproducts that have millimolar affinities for Ca^{2+}. To set the $[Ca^{2+}]_{free}$ at nonactivating levels for physiological processes the [cage] must be more than $[Ca^{2+}]$. Attempts to quantitate the $[Ca^{2+}]_{free}$ waveform under such conditions are shown in Fig. 5. For NP-EGTA, the initial $[Ca^{2+}]_{free}$ = 450 nM, and after laser photolysis this increased to a new steady-state level of $[Ca^{2+}]$ = 17 μM. This irradiation effected approximately 13% cleavage of the total amount of cage present.

Even though Ca-orange-5N is a low-affinity Ca^{2+} indicator, its K_D value for Ca^{2+} is too high to be used to monitor precisely the $[Ca^{2+}]_{free}$ for the first 60 μs after photolysis. Thus, we have modeled the $[Ca^{2+}]$ waveform, assuming that the chelator is cleaved at the rate of decay of the faster *aci*-nitro intermediate for each compound (i.e., 500,000 s^{-1} for NP-EGTA and 80,000 s^{-1} for DM-nitrophen) and that Ca is released by the photoproducts at rate determined by their off rate (k_{4R}, Scheme 3). In the case of NP-EGTA the $[Ca^{2+}]$ transient was estimated to reach a peak value of about 139 μM after 45 μs (Fig. 5, *upper curve*). We have found that the goodness of fit of the model to the detected fluorescence is not very sensitive to, for example, the rate of photolysis (k_2 can vary between 80,000 and 500,000 for NP-EGTA). The fit to the declining phase of the fluorescence was found to be insensitive to the indicator off rate (k_{3R} can vary between 8,000 and 12,600) and the product on rate (k_{4F} can vary between 1.7 and 8.0×10^7); but it is very sensitive to the cage on rate (k_{1F}). Therefore, the modeling should only be considered approximate, as we have not independently measured the on and off rates of the cages or indicator. Such experiments have been carried out with EGTA itself (Smith et al., 1984) and fura-2 (Kao and Tsien, 1988). It was found from rapid stop-flow experiments that the rate constant for Ca^{2+} binding to EGTA was about 1.5×10^6 M^{-1} s^{-1} at pH 7.0. Our values for k_{on} for NP-EGTA and DM-nitrophen were found to be faster than this but less than that of fura-2 (6×10^8 M^{-1} s^{-1}; Kao and Tsien, 1988). This is consistent with the fact that the pK_a values of NP-EGTA and DM-nitrophen (Grell et al., 1989) are intermediate to EGTA and fura-2. Ca^{2+} coordination competes with protons on the nitrogen lone pairs. The time required for Ca^{2+} to effect proton displacement from the nitrogen lone pairs is the reason why the k_{on} of EGTA is less than that of fura-2. The rate of binding of Ca^{2+} to fura-2 is essentially diffusion controlled, because this chelator is unprotonated at physiological pH. Even though we have had to use modeling to gain estimates of the rate constants shown in Table 3, there is good agreement between the Ind:Ca^{2+} signal and its value predicted from the model (Figs. 5 and 6), suggesting that the estimate of peak $[Ca^{2+}]$ obtained in this experiment is reasonable. For NP-EGTA, the peak $[Ca^{2+}]$ is sevenfold higher than the final steady-

state concentration. In the case of DM-nitrophen, the modeling suggests that the peak [Ca^{2+}] is 14-fold higher than the final concentration. The differences between the two predicted Ca^{2+} waveforms in these experiments illustrate how the initial concentrations of cage and Ca^{2+}, rates of photorelease and re-equilibration, pH, and percentage photolysis all affect the time course of the [Ca^{2+}]. It should be noted that the modeling also gives an estimate of the k_{on} for Ca-orange-5N (3×10^8 M^{-1} s^{-1}; Table 3), which is close to the value for fura-2, another BAPTA-based dye, obtained from T-jump experiments (6×10^8 M^{-1} s^{-1}; Kao and Tsien, 1988).

An important question to address in the use of caged Ca^{2+} is what effect large and rapid [Ca^{2+}] transients might have on the process under study. This will of course vary with the properties of each Ca^{2+}-sensing protein. For example, in the case of the ryanodine receptor (RYR) kinetics, Györke and Fill (1993) have shown that the RYR adaptation process they discovered using DM-nitrophen:Ca^{2+} as the caged Ca^{2+} is a result of net release of Ca^{2+} from caged Ca^{2+} (Györke and Fill, 1994) and not a rapid Ca^{2+} pulse (as suggested by Lamb et al., 1994). Furthermore, the channel is not activated when there is rapid Ca^{2+} release without net [Ca^{2+}] release (Györke and Fill, 1994; cf. Valdivia et al., 1995, for analogous experiments with NP-EGTA). The [Ca^{2+}] measurements shown in Figs. 5 and 6 imply that the [RYR:Ca^{2+}] will reach a new steady-state value within 1–2 ms after laser photolysis of either caged Ca^{2+}, about 100-1000 times faster than the time course of receptor adaptation. Recently, Fill and co-workers have demonstrated that Ca-activated K^+ channels are only activated by a net increase in $[Ca^{2+}]_{free}$ and not by a rapid [Ca^{2+}] transient photoreleased from the DM-nitrophen:Ca^{2+} complex (Velez et al., 1995). Rapid Ca^{2+} pulses from DM-nitrophen:Ca^{2+} complex in chromaffin cells also fail to elicit any form of dectectable secretory response (Neher and Zucker, 1993). However, in the giant squid synapse [Ca^{2+}] transients, without net Ca^{2+} release, do evoke powerful transmitter release (Delaney and Zucker, 1990). These few examples of the effects of [Ca^{2+}] transients on various cellular processes illustrate the difficulty of predicting a priori whether or not such rapid photomanipulations of cation concentration will evoke a physiological response.

CONCLUSION

The rate of release of Ca^{2+} from laser flash photolysis of nitrophenyl-EGTA:Ca^{2+} complex was found to be 68,000 s^{-1} at physiological pH when Ca-orange-5N was used as the indicator to monitor the appearance of Ca^{2+}. Examination of the time-dependent absorption changes of the chelator itself resolved two *aci*-nitro signals; the rates of decay of these transients were 500,000 s^{-1} and 100,000 s^{-1}. We believe that the simplest interpretation of these data is that the chelator is cleaved by a mechanism that divides along two parallel paths (giving two *aci*-nitro intermediates), which finally converge to give the same photoproducts (Scheme 1). These products could possibly still carry Ca^{2+} and thus the rate-limiting step in Ca^{2+} release is controlled by cation dissociation from this post-photolysis complex.

The time-dependent increase in fluorescence of Ca-orange-5N upon photolysis of DM-nitrophen:Ca^{2+} was 38,000 s^{-1}, and it too evidenced two *aci*-nitro transient intermediates. These decayed with rates of 80,000 s^{-1} and 11,000 s^{-1}. These rates are both slower than our estimate for the photoproduct dissociation off rate, suggesting that it is chelator fragmentation that is the rate-limiting step in Ca^{2+} release in the case of DM-nitrophen. The data show that both caged calciums can be used to produce large and extremely rapid increases in Ca^{2+} concentration, which can be used to activate Ca^{2+}-dependent physiological processes.

We thank Dr. Robert Fulbright for helping us with the modeling studies and Mr. Alex Fielding for excellent electronic and software support.

This work was supported by the National Institutes of Health (HL40935 to RJB, HL30315 and GM39500 to JHK, and GM53395 to GCRE-D).

REFERENCES

Adams, S. R., J. P. Y. Kao, G. Grynkiewicz, A. Minta, and R. Y. Tsien. 1988. Biologically useful chelators that release Ca^{2+} upon illumination. *J. Am. Chem. Soc.* 110:3212–3220.

Baylor, S. M., W. K. Chandler, and M. W. Marshall. 1982. Use of metallochromic dyes to measure changes in myoplasmic calcium during activity in frog skeletal muscle fibres. *J. Physiol.* 331:139–177.

Billington, A. P., K. M. Walstrom, D. Ramesh, A. P. Guzikowski, B. K. Carpenter, and G. P. Hess. 1992. Synthesis and photochemistry of photolabile *N*-glycine derivatives and effects of one on the glycine receptor. *Biochemistry.* 31:5500–5507.

Corrie, J. E. T. 1993. Synthesis, photochemistry and enzymology of 2-*O*-(2-nitrobenzyl)-D-glucose, a photolabile derivative of D-glucose. *J. Chem. Soc. Perkin Trans.* 1:2161–2166.

Corrie, J. E. T., A. DeSantis, Y. Katayama, K. Khodakhah, J. B. Messenger, D. C. Ogden, and D. R. Trentham. 1993. Postsynaptic activation at the squid giant synapse by photolytic release of L-glutamate from a 'caged' L-glutamate. *J. Physiol.* 465:1–8.

Dantzig, J. A., Y. E. Goldman, N. C, Millar, J. Lacktis, and E. Homsher. 1992. Reversal of the cross-bridge force-generating transition by photogeneration of phosphate in rabbit psoas muscle fibres. *J. Physiol.* 451:247–278.

Delaney, K. R., and R. S. Zucker 1990. Calcium release by photolysis of DM-nitrophen stimulates transmitter release from giant squid synapse. *J. Physiol.* 426:473–498.

Ebashi, S., M. Endo, and I. Ohtsuki. 1969. Control of muscle contraction. *Q. Rev. Biophys.* 2:351–384.

Ellis-Davies, G. C. R., and J. H. Kaplan. 1988. A new class of photolabile chelators for the rapid release of divalent cations: generation of caged Ca and caged Mg. *J. Org. Chem.* 53:1966–1969.

Ellis-Davies, G. C. R., and J. H. Kaplan. 1994. Nitrophenyl-EGTA, a photolabile chelator that selectively binds Ca^{2+} with high affinity and releases it rapidly upon photolysis. *Proc. Natl. Acad. Sci. USA.* 91: 187–191.

Fidler, N., G. C. R. Ellis-Davies, J. H. Kaplan, and J. A. McCray. 1988. Rate of Ca^{2+} release following laser photolysis of a new caged Ca^{2+}. *Biophys. J.* 53:599a.

Grell, E., E. Lewitzki, H. Ruff, E. Bamberg, G. C. R. Ellis-Davies, J. H. Kaplan, and P. De Weer. 1989. Caged-Ca^{2+}: a new agent allowing liberation of free Ca^{2+} in biological systems by photolysis. *Cell. Mol. Biol.* 35:515–522.

Györke, S., and M. Fill. 1993. Ryanodine receptor adaptation: control mechanism of Ca^{2+}-induced Ca^{2+} release in heart. *Science.* 260: 807–809.

Györke, S., and M. Fill. 1994. Ca^{2+}-induced Ca^{2+} release in response to flash photolysis. *Science.* 263:987–988.

Heidelberger, R., C. Heinemann, E. Neher, and G. Matthews. 1994. Calcium dependence of the rate of exocytosis in a synaptic terminal. *Nature.* 371:513–515.

Heuser, J. E., and T. S. Reese. 1981. Structural changes after transmitter release at the frog neuromuscular junction. *J. Cell. Biol.* 88:564–580.

Jackson, A. P., M. P. Timmerman, C. R. Bagshaw, and C. C. Ashley. 1987. The kinetics of calcium binding to fura-2 and indo-1. *FEBS Lett.* 216:35–39.

Kao, J. P. Y., and S. R. Adams. 1993. Photosensitive caged compounds design, properties, and biological applications. *In* Optical Microscopy: Emerging Methods and Applications. B. Herman and J. L. Masters, editors. Academic Press, London. 27–85.

Kao, J. P. Y., A. T. Harootunian, and R. Y. Tsien. 1989. Photochemically generated cytosolic calcium pulses and their detection by fluo-3. *J. Biol. Chem.* 264:8179–8184.

Kao, J. P. Y., and R. Y. Tsien. 1988. Ca^{2+} binding kinetics of fura-2 and azo-1 from temperature-jump relaxation measurements. *Biophys. J.* 53: 635–639.

Kaplan, J. H., and G. C. R. Ellis-Davies. 1988. Photolabile chelators for the rapid photorelease of divalent cations. *Proc. Natl. Acad. Sci. USA.* 85:6571–6575.

Katz, B., and R. Miledi. 1968. The role of calcium in neurotransmitter facilitation. *J. Physiol.* 195:481–495.

Khan, S., F. Castellano, J. L. Spudich, J. A. McCray, R. S. Goody, G. P. Reid, and D. R. Trentham. 1993. Excitatory signaling in bacteria probed by caged chemoeffectors. *Biophys. J.* 65:2368–2382.

Lamb, G. D., M. W. Fryer, and D. G. Stephenson. 1994. Ca^{2+}-induced Ca^{2+} release in response to flash photolysis. *Science.* 263:986.

Llinas, R., M. Sugimori, and R. B. Silver. 1981. Relationship between presynaptic calcium current and postsynaptic potential in squid giant synapse. *Biophys. J.* 33:323–352.

Lu, K. P., and A. R. Means. 1993. Regulation of the cell cycle by calcium and calmodulin. *Endocr. Rev.* 14:40–58.

McClelland, R. A., and S. Steenken. 1987. Pronounced solvent effect on the absorption spectra of the photochemically produced 2,4-dinitrobenzyl carbanion. *Can. J. Chem.* 65:353–356.

McCray, J. A., N. Fidler-Lim, G. C. R. Ellis-Davies, and J. H. Kaplan. 1992. Rate of release of Ca^{2+} following laser photolysis of the DM-nitrophen-Ca^{2+} complex. *Biochemistry.* 31:8856–8861.

McCray, J. A., L. Herbette, T. Kihara, and D. R. Trentham. 1980. A new approach to time-resolved studies of ATP-requiring biological systems: laser flash photolysis of caged ATP. *Proc. Natl. Acad. Sci. USA.* 77: 7237–7241.

Milburn, T., N. Matsubara, A. P. Billington, J. B. Udgaonkar, J. W. Walker, B. K. Carpenter, W. W. Webb, J. Marque, W. Denk, J. A. McCray, and G. P. Hess. 1989. *Biochemistry.* 28:49–55.

Morrison, H., and B. H. Migdalof. 1965. Photochemical hydrogen abstraction by the nitro group. *J. Org. Chem.* 30:3996.

Neher, E., and R. S. Zucker. 1993. Multiple calcium-dependent processes related to secretion in bovine chromaffin cells. *Neuron.* 10:21–30.

Press, W. H., S. A. Teukolsky, W. T. Vetterling, and B. P. Flannery, editors. 1992. Davidson-Fletcher-Powell algorithm for multidimensional minimization. *In* Numerical Recipes in C—The Art of Scientific Computing. Cambridge University Press, New York. 425–430.

Ramesh, D., R. Wieboldt, A. P. Billington, B. K. Carpenter, and G. P. Hess. 1993. Photolabile precursors of biological amides: synthesis and characterization of caged *o*-nitrobenzyl derivatives of glutamine, asparagine, glycinamide, and γ-aminobutyramide. *J. Org. Chem.* 58: 4599–4605.

Schneider, S., M. Fink, and R. Bug. 1991. Investigation of the photorearrangement of *o*-nitrobenzylesters by time-resolved resonance Raman spectroscopy. *J. Photochem. Photobiol. A.* 55:329–338.

Schupp, H., W. K. Wong, and W. Schnabel. 1987. Mechanistic studies of the photorearrangement of *o*-nitrobenzyl esters. *J. Photochem.* 36: 85–97.

Smith, P. D., G. W. Liesengang, R. L. Berger, G. Cerlinski, and R. J. Podolsky. 1984. A stopped-flow investigation of calcium ion binding by ethylene glycol bis(b-aminoethyl ether)-*N,N'*-tetraacetic acid. *Anal. Biochem.* 143:188–195.

Southwick, P. L., and A. S. Waggoner. 1989. Synthesis of purpurate-1,1'-diacetic acid (PDAA) tripotassium salt. A new calcium indicator for biological applications. *Org. Prep. Proc. Int.* 21:493–500.

Valdivia, H. H., J. H. Kaplan, G. C. R. Ellis-Davies, and W. J. Lederer. 1995. Adaptation controls the physiological response of the cardiac ryanodine receptor to calcium. *Science.* 267:1997–2000.

Velez, P., A. L. Escobar, F. Cilfuentes, J. L. Vergara, and M. Fill. 1995. Activation of single Ca^{2+}-activated K^+ chennels by flash photolysis of caged Ca^{2+}. *Biophys. J.* 68:375a.

Walker, J. W., J. Feeney, and D. R. Trentham. 1989. Photolabile precursors of inositol phosphates. Preparation and properties of 1-(2-nitrophenyl-)ethyl esters of *myo*-inositol 1,4,5-trisphosphate. *Biochemistry.* 28: 3272–3280.

Walker, J. W., J. A. McCray, and G. P. Hess. 1986. Photolabile protecting groups for an acetylcholine receptor ligand. Synthesis and photochemistry of a new class of *o*-nitrobenzyl derivatives and their effects on receptor function. *Biochemistry.* 25:1799–1805.

Walker, J. W., G. P. Reid, J. A. McCray, and D. R. Trentham. 1988. Photolabile 1-(2-nitrophenyl)ethyl phosphate esters of adenine nucleotide analogues. Synthesis and mechanism of photolysis. *J. Am. Chem. Soc.* 110:7170–7177.

Wettermark, G. 1962. Photochromism of o-nitrotoluenes. *Nature.* 194:677.

Wieboldt, R., D. Ramesh, B. K. Carpenter, and G. P. Hess. 1994. Synthesis and photochemistry of photolabile derivatives of γ-aminobutyric acid for chemical kinetic investigations of the γ-aminobutyric acid receptor in the millisecond time region. *Biochemistry.* 33:1526–1533.

Wilcox, M., R. W. Viola, K. W. Johnson, A. P. Billington, B. K. Carpenter, J. A. McCray, A. P. Guzikowski, and G. P. Hess. 1990. Synthesis of photolabile precursors of amino acid neurotransmitters. *J. Org. Chem.* 55:1585–1589.

Wootton, J. F., and D. R. Trentham. 1989. "Caged" compounds to probe the dynamics of cellular processes: synthesis and properties of some novel photosensitive P-2-nitrobenzyl esters of nucleotides. *In* NATO ASI Ser. C: Photochemical Probes in Biochemistry. P. E. Nielsen, editor. Kluwer Academic Publishers, Dortrecht. 277–296.

Zhu, Q. Q., W. Schnabel, and H. Schupp. 1987. Formation and decay of nitronic acid in the photorearrangement of *o*-nitrobenzyl esters. *J. Photochem.* 39:317–332.